Inorganic Chemistry

ARTICLE

pubs.acs.org/IC

Palladacycle-Promoted Solvolytic Cleavage of *O,O*-Dimethyl *O*-Aryl Phosphorothioates. Converting a Phosphorane-Like Transition State to an Observable Intermediate

C. Tony Liu, Alexei A. Neverov, and R. Stan Brown*

Department of Chemistry, Queen's University, Kingston, Ontario K7L 3N6, Canada

Supporting Information

ABSTRACT: The mechanism of cleavage of a series of seven *O,O*-dimethyl *O*-aryl phosphorothioates (**6a**−**g**) promoted by a *C,N*-palladacycle, (2-[*N,N*-dimethylamino-(methyl)phenyl]-C^1,N)(pyridine) palladium(II) triflate (**5**:OTf) in methanol at 25 °C was investigated with the aim of identifying catalytically important intermediates. Complete ^s_spH/rate profiles (in methanol) were conducted for the cleavage of **6a**−**g** in the presence of 0.08 mM **5**. The log k_{obs} for the catalyzed methanolysis of **6a** increases linearly with ^s_spH with a plateau above the $^s_s pK_a^1$ of 11.16 for formation of **5**:$^-$OCH$_3$. The profiles for **6b**−**g** are bell-shaped, depending on the apparent ionizations of two acidic groups, with the rate constant maximum of the bell and the $^s_s pK_a^1$ values shifting to higher ^s_spH values as the $^s_s pK_a^{HOAr}$ of the leaving group phenol increases. A Brønsted plot of the log k_{obs}^{max} (the maximum rate constants for cleavage of **6a**−**g**) vs $^s_s pK_a^{HOAr}$ exhibits a downward break at ∼ $^s_s pK_a^{HOAr}$ 13, with the two wings having β_{lg} values of 0.01 and −0.96. A model describing the kinetically important species involves a complex series of equilibria: **5**:(HOCH$_3$):pyr ⇌ **5**:($^-$OCH$_3$):pyr + H$^+$ $\overset{6}{\rightleftharpoons}$ **5**:($^-$OCH$_3$):**6** + pyr ⇌phosphorane **7** → product, where the rate limiting steps change from formation of **5**:($^-$OCH$_3$):**6** to formation of thiophosphorane **7** and then to product formation as the aryloxy leaving groups of **6** get progressively worse. Kinetic experiments indicate that the reaction of **5** with **6e**, having a 4-chlorophenoxy leaving group, rapidly produces a transient intermediate, postulated to be the palladacycle-bound 5-coordinate thiophosphorane (**7e**) that exists long enough to obtain its UV/vis spectrum by stopped-flow spectrophotometry. Detailed analysis of the data sheds light on the origins of a previously reported anomalously large β_{lg} of −1.93 for the descending wing of a Brønsted plot (*J. Am. Chem. Soc.* **2010**, *132*, 16599). Finally, energetics analysis indicates that the binding of palladacycle to the transition state comprising attack of methoxide on **6e**, [MeO$^-$ + **6e**]‡, stabilizes the latter by 34.9 kcal/mol, converting that transition state into an observable intermediate.

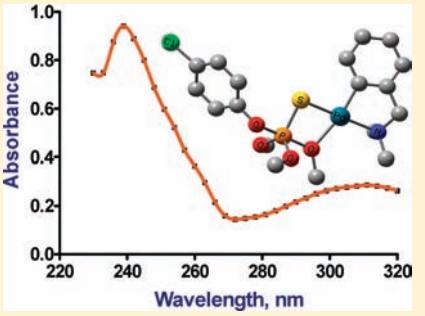

1. INTRODUCTION

Sulfur-containing organophosphate (OP) triesters with a P═S group (known as phosphorothioates) comprise a class of commercially attractive compounds with high toxicity toward insects, mites, and ticks and relatively low mammalian toxicity.[1] Continuing efforts are devoted to developing efficient, novel methods for destruction of OP materials containing the P═O and P═S units. We previously reported that (La^{3+}($^-$OMe))$_2$ and some Zn(II):$^-$OCH$_3$-containing complexes are efficient catalysts for the alcoholysis of phosphate,[2,3] but not phosphorothioate triesters. Catalysts comprising softer metal ions[4,5] such as Cu(II)[6] and formally Pd(I)-containing palladacycles, such as **1**−**4**, have been shown to be efficient at facilitating the hydrolytic cleavage of phosphorothioate triesters[7−9] although in water, catalyst solubility, and product inhibition can decrease the effectiveness considerably.

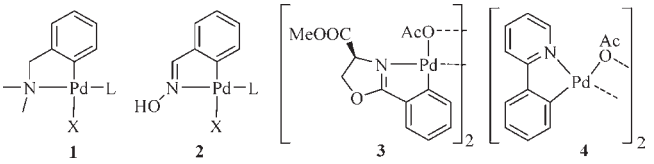

An initial report from our lab[10] and subsequent related ones[11,12] have shown that **5**:(pyr):($^-$OTf) [Pd(II)(2-(*N,N*-dimethylamino-benzylamine)-C^1,N)(pyridine)(triflate)] in methanol under basic conditions immediately forms **5a** (**5**:($^-$OCH$_3$):(pyr)) which gives impressive accelerations of the methanolysis of neutral phosphorothioates (**6**) without marked product inhibition. This is because the **5a**-promoted cleavage of these triesters ((RO)$_2$P═S(OAr)) generates a neutral product ((RO)$_2$P(=S)(OMe)) that binds no more tightly to the catalyst than does the original substrate. A more complete study[13] of the **5a**-catalyzed methanolysis of series **6** (which includes the commercially used OP pesticide fenitrothion (**6c**)) indicated that the catalysis is very efficient: the second order catalytic rate constants (k_2^{cat}) are (1.3−47) × 10^5 greater than the corresponding k_2^{-OMe} rate constants for the methoxide-promoted reactions.

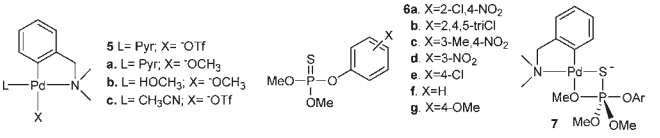

The latter study also indicated that the catalytic process is more complicated than originally thought,[7−12] which necessitated more study to clarify the mechanism of action. In particular, the reported Brønsted plot[13] for the **5a**-catalyzed methanolysis of

Received: May 19, 2011
Published: July 11, 2011

6a−**g** at $^{s}_{s}$pH[14] 11.7 in methanol exhibited a sharp downward break suggestive of a process where there is a change in rate limiting step, implying the existence of one or more intermediates along the reaction pathway. The large negative β_{lg} value of −1.93 for the descending wing of the Brønsted plot is conspicuously large for simple cleavage of the P-OAr bond as it exceeds the theoretical β_{eq} for transfer of the $(MeO)_2P{=}S$ group between oxyanion nucleophiles.[15]

Herein we describe results of detailed kinetic studies of the $^{s}_{s}$pH/rate profiles for cleavage of **6a**−**g** promoted by **5** which indicate there are three changes in rate limiting step in passing from the required active form **5a** to products. This suggests involvement of three essential forms of the palladacycle. These are **5a** and two subsequent complexes having the same stoichiometry, namely, a first formed complex **5**:($^{-}$OCH$_3$):**6**, and a subsequent palladacycle-stabilized 5-coordinate thiophosphorane intermediate, **7**. The latter intermediate, never before observed, is sufficiently stabilized to allow visualization by UV/visible spectrophotometry and determination of the rate constants for its equilibrium formation and breakdown. Finally, we present a detailed analysis that shows that the original large negative coefficient for the steep wing of the Brønsted plot previously reported[13] results from a combination of an equilibrium process (β_{eq} = −1.04) between the starting materials and the thiophosphorane intermediate, and the process involving subsequent leaving group departure with a β_{lg} value of −0.96.

2. EXPERIMENTAL SECTION

2.1.1. Materials and Methods. Sodium methoxide (0.5 M solution in methanol, titrated against N/50 Fisher Certified standard aqueous HCl solution and found to be 0.49 M), tetrabutylammonium hydroxide (1.0 M solution in methanol, titrated to be 1.05 M), Ag(CF$_3$SO$_3$) (99%+), Pd(Cl)$_2$ (≥99.9%), 4-(dimethylamino)pyridine (DMAP, 99%), 2,4,6-collidine (99%), triethylamine (99%), and 2,2,6,6-tetramethylpiperidine (99+%) were obtained from Aldrich. 1-Methylpiperidine (99%) and 1-ethylpiperidine (99%) were obtained from Alfa Aesar and TCI America Laboratory Chemicals, respectively. HClO$_4$ (70% aqueous solution, titrated to be 12.3 M) and *N*,*N*-dimethylbenzylamine (dmba, 99%) were from Acros Organics. Anhydrous methanol was supplied by EMD chemicals. Phosphorothioates **6a**−**g** and catalyst **5** came from an earlier study.[13] ***Caution!*** *All these phosphorothioate substrates are acetylcholinesterase inhibitors and should be handled with great care.*

The $CH_3OH_2^+$ concentrations were determined potentiometrically using a combination glass electrode (Radiometer model XC100−111−120−161) calibrated with Fisher certified standard aqueous buffers (pH = 4.00 and 10.00) as described in a previous paper.[16] The $^{s}_{s}$pH values[14] in methanol were obtained by subtracting a correction constant of −2.24[16] from the electrode readings with the autoprotolysis constant for methanol taken as $10^{-16.77}$ M^2. A listing of the $^{s}_{s}$pK_a values of different substituted phenols in methanol can be found in a previous account.[17]

2.1.2. Preparation of Complex 5c. [Pd(II)(2-(*N*,*N*-dimethylaminobenzylamine)-C^1,N)(CH$_3$CN) (triflate)]. To a stirring solution of 0.377 g (0.686 mmol) of (μ-Cl)$_2$[Pd(dmba)]$_2$ dimer in anhydrous CH$_2$Cl$_2$ (20 mL) was slowly introduced Ag(CF$_3$SO$_3$) (0.355 g, 1.387 mmol) in anhydrous acetonitrile (2 mL). The mixture was allowed to stir at room temperature for 5 min, and the white precipitate formed was removed by filtration. The solvent was removed from the clear filtrate under reduced pressure to yield a yellow solid. The solid was redissolved in ∼1 mL of CH$_2$Cl$_2$, and the complex precipitated out of the solution as a fluffy off-white powder upon the addition of ∼5 mL of pentane. This was washed with 2 × 5 mL portions of pentane and then dried under reduced pressure overnight to give 0.45 g of the complex as white powder in 77% yield. This procedure is similar to the one proposed for the preparation of (μ-CF$_3$SO$_3$)$_2$[Pd(dmba)]$_2$;[18] however, NMR and HRMS analyses confirm the identity of the isolated complex as the acetonitrile-containing complex. In our hands, all attempts to prepare the (μ-CF$_3$SO$_3$)$_2$[Pd(dmba)]$_2$ dimer without acetonitrile in the reaction mixture resulted in rapid formation of palladium black.

Pd(II)(2-(*N*,*N*-dimethylaminobenzylamine)-C^1,N)(CH$_3$CN)(triflate): ^{1}H NMR (400.3 MHz, δ ppm, CD$_3$OD, 25 °C): δ 7.04 (m, 1H), 6.97 (d, J = 7.3 Hz, 1H), 6.90 (m, 2H), 4.01 (s, 2H), 2.76 (s, 6H), 2.08 (br, 3H); ^{19}F NMR (376.5 MHz, δ ppm, CD$_3$OD, 25 °C): δ −81.1; HRMS(ESI+ TOF in MeOH): calcd for C$_{12}$H$_{19}$N$_2$OPd [Pd(II)(2-(*N*,*N*-dimethylaminobenzylamine)-C^1,N)(CH$_3$CN)(HOMe)]: calcd m/z 313.0532 amu; found 313.0559 amu. mp 72−74 °C.

2.2. Kinetics for Reactions Catalyzed by 5. The methanolyses of phosphorothioate triesters **6a**−**g** in the presence of **5** were monitored by UV/vis spectrophotometry at 25.0 °C. In general, a UV-cell (1 cm path length) was charged with 0.05 mM of substrate **6** and a 1−3 mM buffer solution in anhydrous methanol. The latter were composed of various ratios of HClO$_4$ and amines (2,4,6-collidine ($^{s}_{s}$pH = 7.8−8.5), *N*-isopropylmorpholine ($^{s}_{s}$pH = 8.5−9.0), 1-methylpiperidine ($^{s}_{s}$pH = 9.4−9.7), 1-ethylpiperidine ($^{s}_{s}$pH = 9.8−10.5), triethylamine ($^{s}_{s}$pH = 10.9), and 2,2,6,6-tetramethylpiperidine (TMPP; $^{s}_{s}$pH = 11.0−12.2)) to maintain the desired $^{s}_{s}$pH. No inhibition was observed with these buffers between 0.4 and 5.0 mM. For reactions conducted at higher $^{s}_{s}$pH values, 0.5−10 mM of NaOMe was introduced to maintain a constant [$^{-}$OMe]. Reactions were initiated by injecting the appropriate amount of catalyst stock solution into the buffer/substrate mixture so that the final [**5**] = 0.08 mM in 2.5 mL of buffered methanol. The reaction progress was followed by the appearance of the phenolic products at 393 (**6a**), 314 or 390 (**6b**), 320 or 400 (**6c**), 330 or 365 (**6d**), 284 or 292 (**6e**), 273 (**6f**), and 292 nm (**6g**) depending on the $^{s}_{s}$pH. Faster reactions were followed to at least three half-times and fitting the abs. vs time traces to a standard exponential model gave the pseudofirst order rate constants (k_{obs}). Slower processes were studied by initial rate methods. The second order rate constants (k_2^{cat}) for the methanolysis of **6c** promoted by **5** and **5b** (data shown in the Supporting Information, Figures S1 and S2) were determined from fitting the plots of k_{obs} vs [catalyst] to a linear regression forcing the line through the origin. Reported rate constants are the averages of duplicate runs. It is important to point out that when the [catalyst] ≤ [substrate], good first order behavior was found with full release of the expected phenolic product at the end of the reaction, indicating catalyst turnover with no observable product inhibition. This is due to the fact that equilibrium binding of the catalyst and the substrate/product is quite weak,[13] and so the [catalyst] remains constant, satisfying the pseudofirst order conditions. Stock solutions of **5b** (produced from **5c** dissolved in methanol) where the palladacycle exists with either a weakly associated acetonitrile or solvent, develop a light brownish color (indicative of the formation of Pd nanoparticles or palladium black) after two days at room temperature, even with limited exposure to the atmosphere. Thus, these stock solutions were always freshly prepared prior to the kinetic experiments. By contrast, stock solutions of the pyridine-containing palladacycle **5** in neutral methanol are relatively stable, with no signs of color change or loss of reactivity for at least 10 days at room temperature.

2.3. Initial Rate Determination for 5-Catalyzed Methanolyses of 6a and 6c. These were conducted in a UV-cell with TMPP buffer ($^{s}_{s}$pH = 11.6 ± 0.1) and substrates **6a** or **6c** (from 0.01−0.10 mM) in anhydrous methanol. The reactions were initiated by adding aliquots of a methanolic stock solution of **5** to the mixtures which, at this $^{s}_{s}$pH, instantly forms **5a** so that the final [**5a**] and TMPP were 0.08 mM and 2 mM in 2.5 mL of methanol. The appearance of phenoxide products was followed at 400 nm and the first 5−10% of the abs. vs time traces

dx.doi.org/10.1021/ic201062h |*Inorg. Chem.* 2011, 50, 7852–7862

were fit to a standard linear regression to obtain the individual initial rates. The units of the initial rates were first converted to M/s (from abs/min) using the extinction coefficients of the phenoxide products (at 400 nm and $^{s}_{s}$pH = 11.6 ± 0.1, ε = 17600 ± 300 abs/M/cm for 2-chloro-4-nitrophenoxide and ε = 14000 ± 100 abs/M/cm for 4-nitrophenoxide) before being plotted against the [substrate]. The data for **6a** were fit to a standard linear regression (forced through the origin) to give a slope of (0.122 ± 0.002) s^{-1}, which can be converted to a second order rate constant of (1525 ± 30) M^{-1} s^{-1} under the experimental [**5a**] = 0.08 mM. The data for cleavage of **6c** are dealt with in the Results section.

2.4. Spectrophotometric Titration of Palladacycle 5 with Methoxide. A UV-cell was initially charged with 0.1 mM of complex **5** and 0.1 mM NaOMe in methanol (2.5 mL) to generate **5a** in situ. Sequentially, small aliquots of a stock 50 mM solution of NaOMe in methanol were added to the cell. After each addition, the mixture was allowed to equilibrate for ~2 to 6 min to allow the absorbance to stabilize and then the absorbance spectrum from 320−240 nm was collected. The absorbance values at 244 nm (corrected for dilution) were plotted against the [NaOMe] added, and the data were analyzed in two ways using either eq (2S) or eq (4S) as described in Supporting Information. Using the autoprotolysis constant of $10^{-16.77}$ for methanol, the $^{s}_{s}pK_a^2$ value was computed from the titration data. This constant is not a true acid dissociation, but rather a constant relating to the equilibrium displacement of Pd-bound pyridine by methoxide.

3. RESULTS

3.1. $^{s}_{s}$pH/Rate Profiles for the 5-Catalyzed Methanolyses of Phosphorothioate Triesters 6a−g. General observations: The catalytic activity of **5** in methanol is insensitive to added $[CF_3SO_3^-]_{total}$ or $[ClO_4^-]_{total}$ up to 5 mM, and insensitive to $[buffer]_{total}$ from 0.4 mM to 5 mM. At high $^{s}_{s}$pH(≥12) in methanol, **5** decomposes slowly to form Pd black or Pd nanoparticles.[10,11a] The plots of catalytic rate constants (k_{obs}) for cleavage of **6a−g** vs [**5**] are generally linear up to at least 0.08 mM catalyst, after which a slight downward curvature is observed at higher [catalyst]. This is suggested to be due to a common species rate depression caused by a small amount of free pyridine which drives a portion of a catalyst:substrate complex back to the starting materials.[13] At higher $^{s}_{s}$pH saturation kinetics are observed in the k_{obs} vs [catalyst] plots for the less reactive substrate **6e**, consistent with the formation of an intermediate followed by rate-limiting release of the aryloxy leaving group. The $^{s}_{s}$pH/rate profiles (plots of log k_{obs} vs $^{s}_{s}$pH) for the **5a**-catalyzed methanolyses of **6b−g** in Figure 1 exhibit bell-shape profiles, but this is not observed with **6a**. However, the **5b**-promoted cleavage of **6a** does follow a bell-shaped $^{s}_{s}$pH/rate profile (see Supporting Information), indicating that the plateau observed with **6a** results from the presence of pyridine in **5a**. The ascending portions $^{s}_{s}$pH/rate profiles for **6b−d** roughly coincide with that of **6a**. The bell-shaped kinetic data are analyzed by nonlinear least-squares (NLLSQ) fitting of the data to eq 1, derived for the simplified process in Scheme 1, involving two ionizable groups having apparent $^{s}_{s}pK_a^1$ and $^{s}_{s}pK_a^2$ values while accounting for mass balance in [palladacycle]. The $^{s}_{s}pK_a^1$ acid dissociation generates the neutral complex **5a** (of stoichiometry **5**:($^-$OMe):(pyr)) and the $^{s}_{s}pK_a^2$ term relates to a more complex conditional equilibrium for the substitution of the Pd-pyr ligand with methoxide to form an inactive, or far less active, form, **5**:($^-$OMe)$_2$. The k_{obs}^{max} value is the computed maximum catalytic second order rate constant

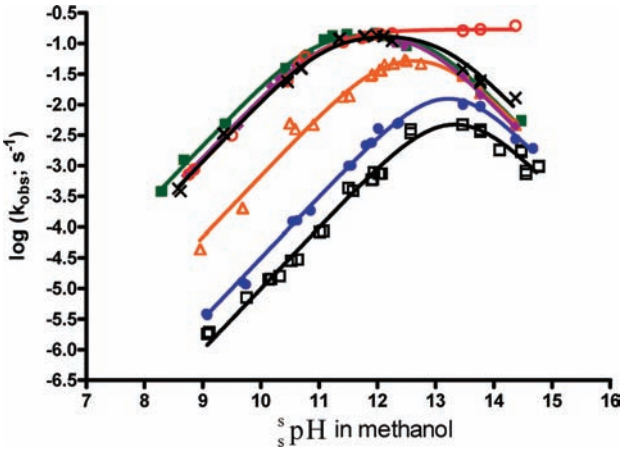

Figure 1. $^{s}_{s}$pH/rate profiles (log k_{obs} vs $^{s}_{s}$pH) for the **5a**-catalyzed methanolyses of 0.05 mM phosphorothioate triesters (**6a**: red open circles, **6b**: ×, **6c**: green solid squares, **6d**: purple solid diamonds, **6e**: orange open triangles, **6f**: blue solid circles, and **6g**: □) in methanol at 25.0 °C, (**5a** = 0.08 mM). The data are fit by a nonlinear least-squares method to the expression in eq 1 to provide the computed $^{s}_{s}pK_a^1$, $^{s}_{s}pK_a^2$, and k_{obs}^{max} values given in Table 1.

Scheme 1. Simplified Process Showing Interconversion of Palladacycle-Bound Species and the Reaction of 5:-($^-$OCH$_3$)(L) with Substrate 6

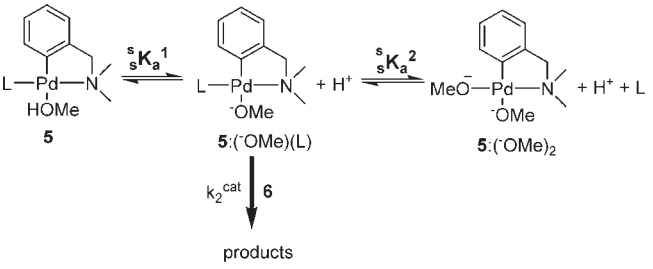

attributed to involvement of **5**:($^-$OMe):(pyr).

$$k_{obs} = \left(\frac{(k_{obs}^{max})(^{s}_{s}K_a^1)[H^+]}{[H^+]^2 + [H^+]\bullet^{s}_{s}K_a^1 + {}^{s}_{s}K_a^1 \bullet^{s}_{s}K_a^2} \right) \quad (1)$$

The maxima of the bell-shaped $^{s}_{s}$pH/rate profiles for triesters **6e−g** are shifted to higher $^{s}_{s}$pH relative to the bell-shaped curves for triesters **6b−d**. In Table 1 are the results obtained from fitting the $^{s}_{s}$pH/k_{obs} kinetic data to eq 1 to obtain $^{s}_{s}pK_a^1$, $^{s}_{s}pK_a^2$, and k_{obs}^{max} values. For the most reactive substrates (**6a−d**) the computed $^{s}_{s}pK_a^1$ and k_{obs}^{max} constants are experimentally the same at ~10.9−11.1 and ~0.16 s^{-1}, respectively. For less reactive substrates (**6e−g**) the k_{obs}^{max} constants progressively decrease and the $^{s}_{s}pK_a^1$ values increase, ultimately by two units to ~12.9 for substrates **6f,g** which have the worst leaving groups. The best fit $^{s}_{s}pK_a^2$ values for the series (excluding **6a**) are between 12.8 and 13.5, but these are mathematically correlated with both the $^{s}_{s}pK_a^1$ and k_{obs}^{max} and have significant errors because of the reduced number of data that define the $^{s}_{s}pK_a^2$ region. Also in Table 1 are the $^{s}_{s}pK_a$ values of the parent phenols,[17] and the k_2^{-OMe} rate constants for the $^-$OCH$_3$-promoted cleavage reactions.[13]

dx.doi.org/10.1021/ic201062h |*Inorg. Chem.* 2011, 50, 7852–7862

Table 1. Computed $^{s}_{s}pK_a^1$, $^{s}_{s}pK_a^2$, and k_{obs}^{max} Constants from NLLSQ Fits of the Kinetic Data of Figure *1* to eq 1 for the 5-Catalyzed Cleavage of 6a−g (0.05 mM) in Methanol at 25.0 °C, along with Second Order Rate Constants (k_2^{-OMe}) for the Methoxide Reactions and $^{s}_{s}pK_a$ Values of the Leaving Group Phenols[a,b]

substrate	6a	6b	6c	6d	6e	6f	6g
$^{s}_{s}pK_a$HOAr	9.35	10.73	11.50	12.41	13.59	14.33	14.77
$^{s}_{s}pK_a^1$	11.16 (±0.03)	11.11 (±0.06)	10.89 (±0.05)	11.08 (±0.03)	12.1 (±0.1)	12.9 (±0.1)	13.0 (±0.2)
$^{s}_{s}pK_a^2$	N.A.	13.15 (±0.07)	12.88 (±0.05)	12.79 (±0.04)	13.2 (±0.1)	13.6 (±0.1)	13.5 (±0.2)
k_{obs}^{max} (s^{-1})	0.169 (±0.006)	0.15 (±0.01)	0.166 (±0.012)	0.165 (±0.009)	0.081 (±0.018)	0.024 (±0.006)	0.011 (±0.004)
k_2^{-OMe} (M^{-1} s^{-1})	(9.3 ± 0.2) × 10^{-3}	(3.9 ± 0.2) × 10^{-3}	(1.05 ± 0.04) × 10^{-3}	(9.1 ± 0.2) × 10^{-4}	(1.22 ± 0.03) × 10^{-4}	(5.1 ± 0.2) × 10^{-5}	(3.5 ± 0.3) × 10^{-5}

[a] Reported errors are standard deviations derived from NLLSQ fitting of the data to eq 1. [b] [**5a**] = 0.08 mM.

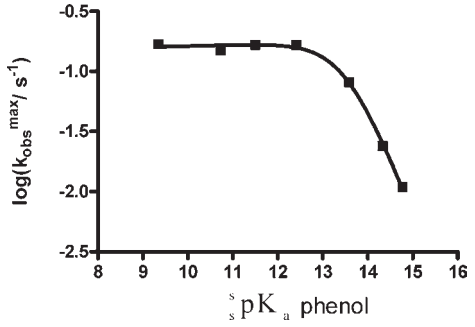

Figure 2. Brønsted plot of log (k_{obs}^{max}) vs $^{s}_{s}pK_a$(phenol) for the **5a**-catalyzed methanolysis of **6a**−**g** (5 × 10^{-5} M) at 25 °C. The line through the data is generated from a NLLSQ fit to the model given in ref 19 to provide two β_{lg} values of 0.01 ± 0.01 and −0.96 ± 0.06; r^2 = 0.9985.

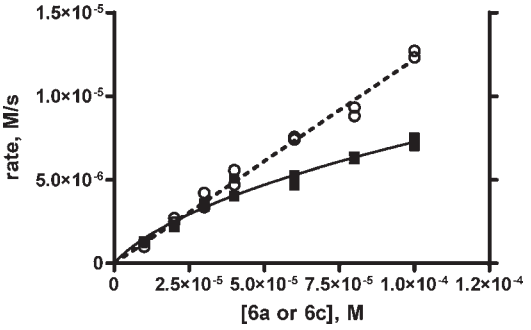

Figure 3. Plot of rates vs [**6a**] (○) or [**6c**] (■) for the catalyzed methanolyses of **6a** and **6c** in the presence of 0.08 mM of **5** and 2 mM of TMPP buffer at $^{s}_{s}$pH = 11.6 ± 0.1 and 25 °C in methanol. The data for **6a** were fitted to a standard linear regression with a slope of (0.122 ± 0.002) s^{-1} while forcing the line through the origin. The data for **6c** were fitted by NLLSQ to the expression defined in eq 4 to give a k_1 value of (2600 ± 700) M^{-1} s^{-1} and r^2 = 0.9608.

3.2. Brønsted Plot for the 5-Catalyzed Methanolyses of Phosphorothioate Triesters 6a−g. The Brønsted plot shown in Figure 2 for the **5a**-catalyzed methanolyses of **6a**−**g** uses the k_{obs}^{max} values and exhibits a downward break at $^{s}_{s}pK_a$ ∼ 13. The data are fit by NLLSQ to an expression[19] for a two-step process with one intermediate, the formation and breakdown of which is subject to a change the rate-limiting step, and two β_{lg} values of β^1_{lg} = 0.01 ± 0.01 and β^2_{lg} = −0.96 ± 0.06. This can be compared with the plot previously constructed[13] on the basis of the observed k_2^{cat} values (defined as $k_{cat}/[\mathbf{5}]$) at a single $^{s}_{s}$ pH of 11.7 for the same reaction having β^1_{lg} = 0.01 and β^2_{lg} = −1.93.

3.3. Initial Rate Determination for 5a-Catalyzed Methanolyses of 6a and 6c. Figure 3 gives initial rate data at $^{s}_{s}$pH = 11.6 ± 0.1 and 25 °C as a function of [**6a**] or [**6c**]. At a total [**5a**] of 0.08 mM, the data for **6a** fit a linear regression providing a k_{obs} of 0.122 s^{-1} giving a second order rate constant of $k_{obs}/[\mathbf{5a}]$ = 1525 ± 30 M^{-1} s^{-1}. The plot for **6c** is downward curved, indicative of a different behavior than with **6a**. Comparison of the two plots suggests a single bimolecular rate limiting step for reaction of **6a** and a change in rate limiting steps in the cleavage of **6c** involving the equilibrium formation of a **5**:**6c** complex and its subsequent breakdown. This is analyzed in terms of the simplified process in eq 2, which describes a kinetic process involving an equilibrium (k_1/k_{-1} = K_1) followed by a rate limiting k_2 term for the formation of a second intermediate, proposed to be a palladacycle-bound 5-coordinate thiophosphorane intermediate, **7**. Steady state treatment in [**5**:**6c**] gives the middle term of eq 3, but because the amount of pyridine produced will be equal to that of **5**:**6c**, further mathematical manipulation generates the right-hand term of eq 3. The rate of formation **7** from the unimolecular reaction of **5**:**6c** is described by eq 4 which was used to fit the initial rate data for substrate **6c**, giving a computed k_1 value of (2600 ± 700) M^{-1} s^{-1}.

$$\mathbf{5} + \mathbf{6c} \underset{k_{-1}}{\overset{k_1}{\rightleftharpoons}} \mathbf{5{:}6c} + \text{py} \xrightarrow{k_2} \mathbf{7} \quad (2)$$

$$[\mathbf{5{:}6c}] = \frac{k_1[\mathbf{5}][\mathbf{6c}]}{k_2 + k_{-1}[\text{pyr}]} = \frac{-k_2 + \sqrt{k_2^2 + 4k_{-1}k_1[\mathbf{5}][\mathbf{6c}]}}{2k_{-1}} \quad (3)$$

$$\text{rate} = k_2[\mathbf{5{:}6c}] = \frac{k_2(-k_2 + \sqrt{k_2^2 + 4k_{-1}k_1[\mathbf{5}][\mathbf{6c}]})}{2k_{-1}} \quad (4)$$

Unfortunately, the k_2 and the k_{-1} terms in eq 4 are heavily correlated so that only the ratio of k_2/k_{-1} (∼3 × 10^{-6} M) can be estimated with any confidence. Nevertheless, the data for **6c** show the anticipated square root dependence for the concentration vs rate profile in Figure 3.

3.4. Saturation Behavior for Plot of k_{obs} vs [5] for the Cleavage of 6e. The catalytic cleavage of **6e**, lying on the descending wing of the Brønsted plot in Figure 2, was investigated as a function of [**5**] at $^{s}_{s}$pH values of 11.7, 12.1, and 12.4. In Figure 4 are the three k_{obs} vs [**5**] plots indicative of saturation behavior which, when analyzed in terms of a universal binding model,[20] indicate the formation of an intermediate **5**:**6e** complex with a $^{s}_{s}$pH dependent conditional dissociation constant of K_{dis} = (6.8−15.5) × 10^{-5} M and a unimolecular breakdown rate

dx.doi.org/10.1021/ic201062h |*Inorg. Chem.* 2011, 50, 7852–7862

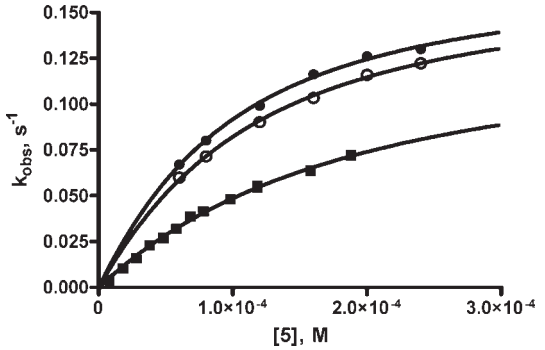

Figure 4. Plot of k_{obs} vs [**5**] for the catalyzed methanolysis of **6e** (5×10^{-5} M) in the presence of 2 mM TMPP buffer at $^{s}_{s}$pH 11.7 ± 0.1 (■), 12.1 ± 0.1 (○), and 12.4 ± 0.1 (●) at followed at 292 nm and 25.0 ± 0.1 °C in anhydrous methanol. The data points are fit[20] to give the following constants. (■): log K_{cond} =3.81 ± 0.04, k_{max} = 0.140 ± 0.006 s^{-1}, r^2 = 0.9975; (○): log K_{cond} = 4.08 ± 0.03, k_{max} = 0.172 ± 0.004 s^{-1}, r^2 = 0.9981; (●): log K_{cond} = 4.17 ± 0.04, k_{max} = 0.175 ± 0.005 s^{-1}, r^2 = 0.9967. (K_{cond} is a conditional binding constant which is the reciprocal of K_{dis} determined at the three $^{s}_{s}$pH values.).

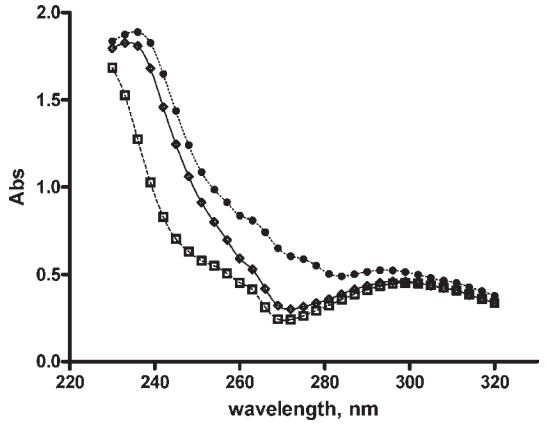

Figure 5. Plots of absorbance vs wavelength for a mixture containing 0.4 mM **5b**, 0.2 mM **6e**, and 2 mM of TMPP buffer ($^{s}_{s}$pH 12.0 ± 0.1) at 0.005 s (□---□), 0.105 s (◇——◇), and 20 s (●····●) after stopped-flow mixing in methanol at $^{s}_{s}$pH 12.0 ± 0.1 and 25 °C. Spectral data points are acquired every 3 nm.

constant for the production of phenol product of 0.17–0.18 s^{-1}. In the Supporting Information, Figure 3S is a similar plot of the decomposition of **6e** in the presence of increasing [**5b**] (which does not contain pyridine) at $^{s}_{s}$pH 12.0, having a K_{dis} of 7.4 × 10^{-5} M and a unimolecular breakdown rate constant of 0.22 s^{-1}.

3.5. Further Evidence for the Formation of Phosphorane 7e from Reaction of 5b with 6e. A stopped-flow reaction analyzer was used to determine the spectral changes from 230 to 320 nm that accompany the conversion of **6e** to its product phenol in the presence of **5b**. Mixing equal volumes of two solutions containing 0.4 mM of **6e** with 4.0 mM of TMPP buffer and 0.8 mM of palladacycle **5b** in methanol instantly forms a mixture at $^{s}_{s}$pH 12.0 ± 0.1 containing half the initial concentrations, from which the spectra were determined as a function of time. Shown in Figure 5 are spectra determined after 0.005, 0.105, and 20 s which respectively correspond to the starting mixture, equilibrium formation of what we contend is the palladacycle-bound thiophosphorane **7e**, and the final product mixture. The equilibrium formation of **7e**, which has a large increase in absorbance at 240 nm, is attained within 0.05 s, being formed with a $k_{formation}$ = 87 s^{-1} under these conditions.

The UV–vis spectrum of **7e** can be constructed by subtracting the spectra of the reaction mixture at 0.005 s from that at 0.105 s. Complex **7e** is not fully formed under these conditions, but its concentration can be estimated from the saturation kinetics curve observed for the **5b**-catalyzed methanolysis of **6e** given in the Supporting Information, Figure 3S. At [**5b**] = 0.4 mM and [**6e**] = 0.2 mM, intermediate **7e** is ~80% formed allowing us to estimate the ε at λ_{max} = 239 and 311 nm. The UV–vis spectrum in Figure 6 of ~80% (~0.16 mM) Pd-bound **7e** in methanol was constructed by adding the spectra of 0.16 mM of **5b** and 0.16 mM of **6e** in methanol to the differential spectrum described above. By way of comparison, a spectrum of the palladacycle bound to an anionic phosphorothioate diester, **8**, formed from 0.16 M each of **5c** and *O*-methyl *O*-phenyl phosphorothioate[21] in methanol, is given in the Supporting Information. Complex **8** is fully formed under these conditions,[21] and its spectrum of complex **8** exhibits

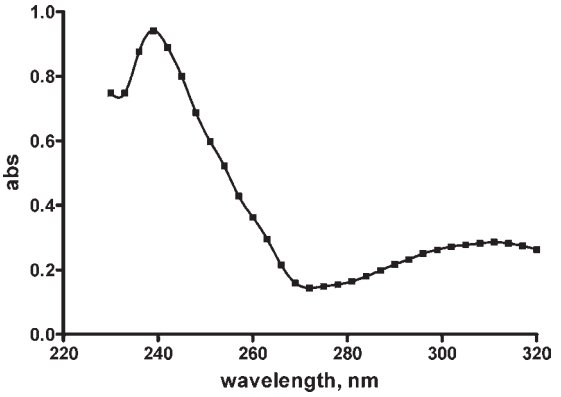

Figure 6. UV/vis spectrum of 0.16 mM **7e** in buffered methanol, $^{s}_{s}$pH 12.0 ± 0.1, determined from difference between spectra of starting materials and equilibrium mixture formed after 0.105 s shown in Figure 5. Extinction coefficients of 5886 M^{-1} cm^{-1} and 1790 M^{-1} cm^{-1} at λ_{max} = 239 and 311 nm were obtained as described in the Text. Spectral data were acquired every 3 nm.

peaks at 226 nm (ε = 14870 M^{-1} cm^{-1}) and 326 nm (ε = 1150 M^{-1} s^{-1}) with no additional peaks out to 700 nm.

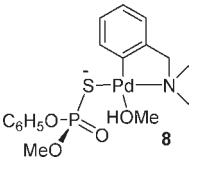

8

3.6. Spectrophotometric Titration for the Determination of the $^{s}_{s}pK_a^2$ Value. To provide experimental data for the **5**:($^{-}$OMe):(L) + $^{-}$OMe ⟷ **5**:($^{-}$OMe)$_2$ + L equilibrium proposed in Scheme 1, spectrophotometric titrations of a 0.1 mM solution of **5** and enough NaOMe in methanol to generate the species **5a** (**5**:($^{-}$OMe):(pyr)) in situ were undertaken as described in the Supporting Information. Small aliquots of a 50 mM stock solution of NaOMe in methanol were added to the cell, and the solutions were allowed to equilibrate for ~2 to 6

dx.doi.org/10.1021/ic201062h |*Inorg. Chem.* 2011, 50, 7852–7862

Scheme 2. Proposed Ionization Events Likely to Be Involved in the Palladacycle 5-Catalyzed Cleavage of Phosphorothioate Triesters 6 in Methanol: L = pyr, OR = OCH_3

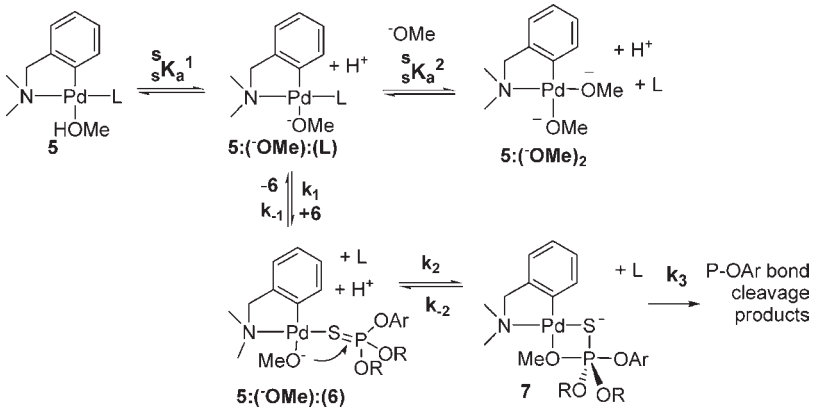

min after which the spectrum from 320−240 nm was collected. Figure 6S (Supporting Information) shows the absorbance values at 244 nm (corrected for dilution) plotted against the added [NaOMe]. The data were analyzed in two ways by NLLSQ fitting to eq (2S) and eq (4S), (Supporting Information). The calculated average $^{s}_{s}pK_a^2$ values for **5** (eq (2S) of 13.3 and eq (4S) 13.2, Supporting Information) are close to the average of the kinetically derived values reported in Table 1 for substrates **6b**−**g**.

4. DISCUSSION

There are five observations of note which are interpreted to support the working model outlined in Scheme 2 for the mechanism of cleavage of **6** promoted by **5**. These are as follows: (1) the large negative β_{lg} value of −1.93 observed for the Brønsted plot in ref 13; (2) the appearance of the $^{s}_{s}$pH/rate profiles given in Figure 1, and in particular the apparent shift to higher $^{s}_{s}$pH for both $^{s}_{s}pK_a^1$ and the maxima of the bell-shaped profiles; (3) the different behavior of the initial rate profiles shown in Figure 3 for cleavage of **6a** and **6c** in the presence of a constant [**5**]; (4) the saturation kinetics for the plot of k_{obs} vs [**5**] shown in Figure 4 for methanolysis of **6e** promoted by **5**; and (5) the fast buildup and then slower decline of an intermediate (**7e**) produced during the **5b**-promoted cleavage of **6e**. We will deal with these in turn.

4.1. Palladacycle 5-Catalyzed Methanolyses of Triesters 6a−g. The original Brønsted plot[13] was constructed from the apparent second order rate constant, k_2^{cat}, data for **5**-promoted cleavage of **6a**−**g** (5×10^{-5} M) at one $^{s}_{s}$pH of 11.7 in methanol at 25 °C. This $^{s}_{s}$pH was chosen as it is ∼1 unit higher than the previously reported $^{s}_{s}pK_a$ of 10.8−11.0 for the acid dissociation constant of **5**:(HOMe):(pyr) forming **5**:($^{-}$OMe):(pyr).[10−12] The general shape of that plot, with its downward break at $^{s}_{s}pK_a$ ∼ 13, is similar to the new Brønsted plot in Figure 2 determined with the k_{obs}^{max} values for decomposition of **6a**−**g** calculated at the maximum of each substrate's $^{s}_{s}$pH/rate profile in the presence of 0.08 mM **5**. The former β_{lg} value of −1.93 ± 0.06 is more negative than that in Figure 2 (β_{lg} = −0.96), conspicuously so since the β_{eq} value for equilibrium transfer of $(MeO)_2P{=}S$ group between oxyanion nucleophiles in methanol is −1.39.[15,22]

The reason for the discrepancies in β_{lg} is now apparent from inspection of the individual $^{s}_{s}$pH/rate profiles in Figure 1. Although the rate constants acquired[13] for catalytic cleavage of **6a**−**d** at $^{s}_{s}$pH 11.7 are in a pH-independent region, for substrates **6e**−**g** they are in the ascending wing of the $^{s}_{s}$pH/rate profiles. A vertical slice through the $^{s}_{s}$pH/rate profile at $^{s}_{s}$pH 11.7 amplifies the differences between the rate constants when it intersects the profiles of substrates at the ascending portion of their $^{s}_{s}$pH/rate profile, leading to the large negative β_{lg} value. As will be shown, the large β_{lg} is a consequence of a mechanism that involves equilibria between at least three intermediates with changes in rate limiting steps that are visualized by varying the substrates' leaving groups.

4.2. Qualitative Description of the pH/Rate Profiles in Figure 1 and Brønsted Plot in Figure 2. The downward break in the Figure 2 Brønsted plot signifies a change in rate limiting step requiring one or more intermediates along the catalytic reaction pathway. The model proposed in Scheme 2 has two kinetically important intermediates of the same stoichiometry, **5**:($^{-}OCH_3$):**6** and **7**, with P-OAr bond cleavage of the latter being rate limiting for **6e**−**g**. The Scheme also suggests that substrates **6** and $^{-}$OMe compete for the Pd-center of **5**, displacing the L (pyridine in the case of **5a**, methanol in the case of **5b**). The **5**:($HOCH_3$):(L) ⇌ **5**:($^{-}OCH_3$):(L) + H^+ ionization is coupled with the equilibrium binding of **6** and formation of **7** leading to product. Palladacycle **5** is also converted to an inactive form (**5**:($^{-}OCH_3)_2$) at higher $^{s}_{s}$pH, formed by equilibrium displacement of pyridine from **5** by methoxide, accounting for the descending wings of the $^{s}_{s}$pH/rate profiles.

The $^{s}_{s}$pH/rate profiles in Figure 1 can be divided into three groups, each of which fits with the Scheme 2 mechanism. The sole member of the first group is **6a** where the k_{obs}^{max} plateaus between $^{s}_{s}$pH ∼ 11.5 and ∼14.5. We suggest that, under the concentration regimes studied here, the **5**-catalyzed reaction of **6a** is limited by a kinetically irreversible ligand substitution step (k_1). The fact that the initial rate data with **6a** shown in Figure 3 are linear, suggests this is a true second order process under the conditions investigated, forming **5**:($^{-}OCH_3$):**6a** which undergoes fast intramolecular cyclization to form thiophosphorane **7a** and then product. In this case the rate of **6a**/pyridine ligand exchange greatly exceeds (by ∼400 times) the rate of displacement of pyridine from **5**:($^{-}OCH_3$):(pyr) by CH_3O^- (apparent k_2 values 2100 and 5.1 M^{-1} s^{-1})[23] accounting for the plateau from $^{s}_{s}$pH ∼11.5 to ∼14.5.

The second group, with close overlapping bell-shaped $^{s}_{s}$pH/rate profiles in Figure 1 comprises **6b**−**d**, where the

dx.doi.org/10.1021/ic201062h |Inorg. Chem. 2011, 50, 7852–7862

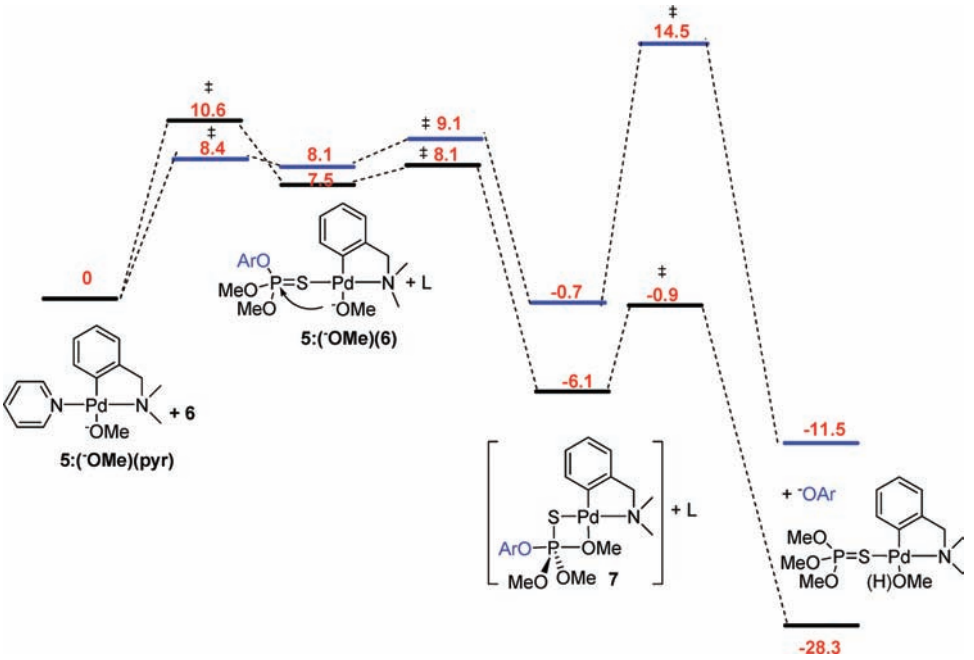

Figure 7. DFT computed reaction pathway for the **5a**-catalyzed methanolyses of phosphorothioates **6c** (OAr = 3-methyl 4-nitrophenoxy; black lines) and **6g** (OAr = 4-methoxyphenoxy; blue lines) resketched and modified from the diagram in ref 13. The red numbers are the $\Delta G^{\ddagger}_{corr}$[24] values in methanol at 25 °C in units of kcal/mol; diagram is to scale.

electrophilicity of the P═S unit systematically decreases because of the change in leaving group. This results in a progressively higher barrier for the rate-limiting intramolecular nucleophilic attack k_2 step to generate **7**. The result is that **5**:($^{-}$OCH$_3$):**6b**−**d** are in equilibrium with **5**:($^{-}$OMe):(pyr), **5**:(HOMe):(pyr), and the **5**:($^{-}$OMe)$_2$ species, accounting for the onset of the descending high $^{s}_{s}$pH wing of the bell-shaped profiles for these substrates ($^{s}_{s}pK^{2}_{a}$ of ∼12.9). The initial rate experiment (Figure 3) with **6c** shows a downward curvature with a square root dependence on [**6**], consistent with kinetics involving the equilibrium ($k_1/k_{-1} = K_1$) formation of **5**:($^{-}$OCH$_3$):**6c** followed by a rate limiting k_2 kinetic step.

The third group comprises **6e**−**g**, where there is equilibrium formation of **7**, followed by rate limiting P-OAr bond scission (k_3). This is consistent with the catalytic k_{obs}^{max} for **6e**−**g** being quite sensitive to the $^{s}_{s}pK_a$ of the leaving group phenols. A density functional theory (DFT) computed energy diagram at standard state of 1 M illustrated in Figure 7 for two substrates where the leaving group is good (**6c**) and bad (**6g**) shows that, as the leaving group becomes worse, the energy barrier for P-OAr bond cleavage increases to the point where this becomes rate-limiting, as is the case for substrates **6e**−**g**. The palladacycle-bound thiophosphorane **7** formed from **6g** sits just −0.7 kcal/mol[13] below **5**:($^{-}$OCH$_3$):(pyr) while that formed from **6c** is −6.1 kcal/mol lower. For **6e**−**g** all the events prior to the cleavage of thiophosphorane **7** are pre-equilibria, so the observed kinetic constant is a product of two equilibrium constants and kinetic constant. An interesting consequence of the catalytic methanolysis of **6e**−**g** is that the apparent $^{s}_{s}pK^{1}_{a}$ values are the products of all the equilibrium processes between **5**:($^{-}$OCH$_3$):(pyr) and **7**. In fact, the change in the kinetic $^{s}_{s}pK^{1}_{a}$ value observed in this study is a useful indicator of the existence of a kinetically relevant intermediate(s) lying between products and **5**:($^{-}$OCH$_3$):(pyr).

4.3. Origin of the Large β_{lg} Value for the Departure of Leaving Groups during the 5-Promoted Cleavage of Phosphorothioates

Scheme 3. Equations for the Formation and Breakdown of 7

$$\text{5:(HOMe):(pyr)} \overset{(^{s}_{s}K_a{}^{1})^{t}}{\rightleftharpoons} \text{5:(}^{-}\text{OMe):(pyr)} + \text{H}^{+} \quad (5)$$

$$\text{5:(}^{-}\text{OMe):(pyr)} + \mathbf{6} \underset{k_{-1}}{\overset{k_1}{\rightleftharpoons}} \text{5:(}^{-}\text{OMe):6} + \text{pyr} \quad (6)$$

$$\text{5:(}^{-}\text{OMe):6} \underset{k_{-2}}{\overset{k_2}{\rightleftharpoons}} \mathbf{7} \quad (7)$$

$$\text{5:(HOMe):(pyr)} + \mathbf{6} \overset{K_B}{\rightleftharpoons} \mathbf{7} + \text{H}^{+} + \text{pyr} \quad (8)$$

$$\mathbf{7} \xrightarrow{k_3} \text{products} \quad (9)$$

6d−**g.** *4.3.1. Brønsted Gradient (β) for the Formation of Thiophosphorane 7.* Having shown from spectrophotometric titrations and kinetics that the descending wings result from the formation of inactive, or weakly active **5**:($^{-}$OCH$_3$)$_2$, we do not consider its presence further in developing the simplified kinetic expressions derived below. We note, however, that the $^{s}_{s}pK^{2}_{a}$values in Table 1 for **6e**−**g** appear to be slightly larger than for **6b**−**d**. There is no obvious reason that the former values should be different from the latter, and because of the relatively large errors, no further discussion is attempted.

Given in eqs (5−9) of Scheme 3 are simplified equations based on the general process in Scheme 2 describing the equilibrium formation of **7** (without the complicating $^{s}_{s}pK^{2}_{a}$ process), followed by its breakdown to products. At a constant and small [pyr] (as is the case here), common species rate depressions by pyridine are not evident in the kinetics of the catalyzed reactions when the total concentration of **5** is ≤0.08 mM, so we can simplify the treatment further by considering that the [pyr] is constant at a set [**5**], and slight changes in its concentration do not greatly affect the kinetic behavior.

For **6a**, where the rate limiting step is binding of substrate to **5**:($^{-}$OCH$_3$):(pyr) (the k_1 step of eq (6)), the reaction is

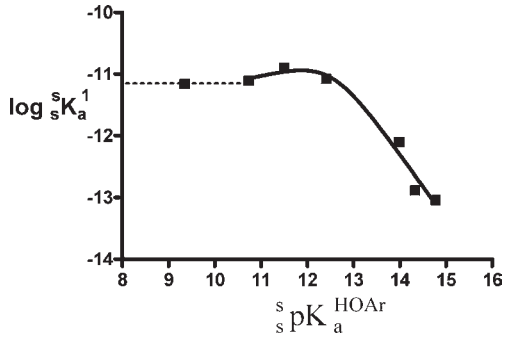

Figure 8. Plot of log $^{s}_{s}K^{1}_{a}$ vs $^{s}_{s}pK^{HOAr}_{a}$ for the catalyzed cleavages of **6a**−**g** (5×10^{-5} M) at 25 °C in methanol. The log $^{s}_{s}K^{1}_{a}$ values are derived from Table 1 for [**5**] = 0.08 M. The line through the data is generated from a NLLSQ fit to the model given in ref 19 to provide two β_B values of 0.17 ± 0.38 and −1.04 ± 0.17; r^2 = 0.9767.

controlled by the ionization of **5**:($HOCH_3$):(pyr) with the thermodynamic acid dissociation constant $(^{s}_{s}K^{1}_{a})^{t}$. For **6b**−**d** where there is equilibrium formation of **5**:($^{-}OCH_3$):**6b**−**d**, the observed rate constant is given as k_2[**5**:(HOMe):(pyr)] $(K_1(^{s}_{s}K^{1}_{a})^{t}/([H^+] + K_1(^{s}_{s}K^{1}_{a})^{t}))$. In these cases, the observed kinetic $^{s}_{s}K^{1}_{a}$ is an apparent acid dissociation constant that is a product of an equilibrium constant (K_1) and $(^{s}_{s}K^{1}_{a})^{t}$. The effect of changes in the substrate leaving groups on $^{s}_{s}K^{1}_{a}$ manifests itself in a slightly positive β value when plotted vs $^{s}_{s}pK^{HOAr}_{a}$ as in Figure 8 (which will be further described below). The observations that the three substrates **6b**−**d** give a β = 0.17 ± 0.38 (Figure 8) suggests not only that the pyridine displacement constants, k_1 and K_1, have a weak dependence on the leaving group ability as measured by $^{s}_{s}pK^{HOAr}_{a}$, but that when coupled with slightly negative dependence for intramolecular attack for the k_2 term,[25] produces an overall insensitivity for the K_1k_2 term.

For less reactive substrates **6e**−**g**, the rate-limiting step of the reaction is the breakdown of intermediate **7** (step k_3). Consequently, for **6e**−**g** all the preceding steps are considered to be at equilibrium, with the constant K_B = [**7**][H^+]/([**5**:(HOMe):(pyr)][**6**]) describing the sum of the steps in eqs (5−7) in Scheme 3. Numerically, $K_B = K_1K_2$ $(^{s}_{s}K^{1}_{a})^{t}$, where $K_1 = k_1/k_{-1}$ and $K_2 = k_2/k_{-2}$. Of these, only K_2 is expected to be heavily dependent on the electronic properties of the phosphorothioate's leaving group since this is the only equilibrium step where a significant change in the P-OAr bonding occurs. The equilibrium position between free **6** plus **5**:(HOMe):(pyr) and the intermediate **7** is inversely dependent on [H^+], since the ratio [**7**]/[**6**] = $(K_2/[H^+])([\mathbf{5}\text{:(HOMe):(pyr)}]K_1(^{s}_{s}K^{1}_{a})^{t})$ = $(K_B[\mathbf{5}\text{:(HOMe):(pyr)}])/[H^+]$. Because K_2 becomes smaller as the leaving group becomes worse, less [H^+] (or more [^{-}OMe]) is required to maintain the same [**7**]/[**6**] ratio at a constant [**5**:(HOMe):(pyr)]. This is consistent with the observed upward shift in the kinetic $^{s}_{s}pK^{1}_{a}$ in Figure 1 (Table 1). Put another way, the computed $^{s}_{s}pK^{1}_{a}$values in Table 1 represent the [H^+] required to keep [**7**] = [**6**], and under this condition K_B[**5**:(HOMe):(pyr)] = [H^+].

In Figure 8 is a plot of the observed kinetic $^{s}_{s}pK^{1}_{a}$ vs $^{s}_{s}pK^{HOAr}_{a}$. The solid line is calculated from an unrestricted fit of the data for **5**-promoted cleavage of **6b**−**g** to a model having a single break,[19] with two β_B values: one of these of 0.17 ± 0.38 for formation of **7** from **5** and **6b**−**d**, and the second is −1.04 ± 0.17 for formation of **7** from **5** and **6e**−**g**. The datum for **6a**, a substrate different from the others because it has no equilibrium binding to the catalyst, is included on the graph but is not used for the fitting. A horizontal dotted line through that point intersects the *Y*-axis at $(^{s}_{s}K^{1}_{a})^{t}$ = 11.16 ± 0.03. For **6b**−**d** where the reaction involves equilibrium binding of substrate followed by rate limiting k_2 cyclization of **5**:($^{-}OCH_3$):**6b**−**d**, we can make a suggestion that the slightly positive β_B stems from weaker binding for substrates with low $^{s}_{s}pK^{HOAr}_{a}$ leaving groups because of their electron withdrawing properties. Positive respective β_B values of 0.96 and 0.49 for binding of substituted phenoxides with Yb^{3+}[26a] and La^{3+}[26b] have been observed previously. These are larger than what is seen here because the phenoxides were directly coordinated to the highly positively charged Ln^{3+} ions, so the effect of substituent is much more pronounced than it is for the binding of **6b**−**c**. Finally, substrates **6e**−**g** react through equilibrium binding and cyclization to form **7** followed by rate-limiting expulsion of the leaving group (k_3), so the β_B of −1.04 is indicative of a binding process which involves a large change in the P-OAr bonding.

*4.3.2. Large β_{lg} Includes Effects of the Leaving Group on Equilibrium Formation of **7** and Its Subsequent Decomposition.* The concentration of the Pd-bound thiophosphorane can be expressed as [**7**] = $[\mathbf{6}]_{total}\cdot(K_B[\mathbf{5}])/([H^+] + K_B[\mathbf{5}])$ after accounting for material balance of [**7**] + [**6**] = $[\mathbf{6}]_{total.}$ Accordingly, the rate of the reaction for the catalyzed methanolyses of **6e**−**g** is described by eq 10 where K_B is the overall equilibrium constant defined in eq (8) above, and the expression for the pseudofirst order rate constant for product formation at a given $[\mathbf{6}]_{total}$ and constant [**5**] (assuming a constant and small [pyridine]) is given in eq 11. Equation 11 indicates that the equilibrium formation of **7** depends on the $^{s}_{s}$pH of the reaction and at lower [H^+], or higher [$^{-}OCH_3$], the k_{obs} value approaches the k_3 limit.

$$\text{Rate} = k_3[\mathbf{7}] = k_3[\mathbf{6}]_{total}\cdot(K_B[\mathbf{5}])/([H^+] + K_B[\mathbf{5}]) \quad (10)$$

$$k_{obs} = k_3(K_B[\mathbf{5}])/([H^+] + K_B[\mathbf{5}]) \quad (11)$$

This trend is confirmed in Figure 4 which depicts the saturation kinetics of **5**-promoted decomposition of **6e**, and where the observable conditional binding constant (K_{cond}) for the formation of **7** becomes larger under more basic conditions. Extrapolation of the data in Figure 4 also indicates that while the conditional binding constant changes as a function of $^{s}_{s}$ pH, within the experimental limits the k_{obs}^{max} does not. This is expected since k_{obs}^{max} represents the k_3 constant for the decomposition of **7e** that is obtained from substrate **6e** plus **5a**. Accordingly, saturation kinetics are seen for the **5b**-catalyzed methanolysis of **6e** (0.05 mM) at $^{s}_{s}$pH 12.0 ± 0.1 and 25 °C (Supporting Information, Figure 3S). Although **5b** contains no Pd-bound pyridine, thiophosphorane **7e** formed from it prior to the k_3 bond cleavage step is the same as the one generated from **5a**. In fact the k_{obs}^{max} value of 0.220 ± 0.006 s^{-1} determined for the **5b**-catalyzed cleavage of **6e** matches well with the ~0.17 s^{-1} seen for methanolysis of **6e** promoted by **5**. The fact that these rate constants are very similar supports our previous assumption (vide supra) that, under the conditions chosen, the presence of pyridine does not greatly affect the overall kinetic behavior.

Interestingly enough, the origin of the discrepancy between the Brønsted β_{lg} of −0.96 reported here (Figure 2) and the β_{lg} of −1.93 previously discussed[13] is understandable from inspection of eq 11. At one extreme, under high $^{s}_{s}$pH conditions where the buildup of intermediate **7** is significant (where the maximum rate constant, k_{obs}^{max}, is achieved in Figure 1), eq 11 can be simplified as $k_{obs} = k_3 = k_{obs}^{max}$ at a given [**5**]. Therefore, when the log

dx.doi.org/10.1021/ic201062h |*Inorg. Chem.* 2011, 50, 7852–7862

Scheme 4. Thermodynamic Cycle for Comparing the Palladacycle 5:$(HOCH_3)_2$-Promoted Reaction and the Methoxide-Promoted Reaction for Substrate 6e[a]

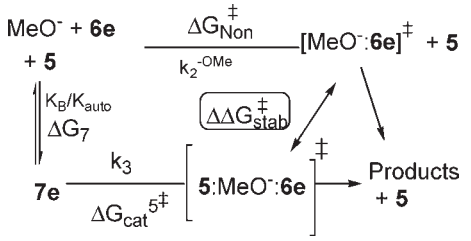

[a] For simplification of the diagram, 5:$(HOCH_3)_2$ is designated as 5.

(k_{obs}^{max}) is plotted against the ${}^{s}_{s}pK_a^{HOAr}$ as in Figure 2, the β_{lg} value determined is strictly a measure of the sensitivity of the bond cleavage to the nature of the leaving group in the k_3 process. On the other hand, the previously reported β_{lg} value of −1.93 is determined from taking a vertical slice of ${}^{s}_{s}pH$/rate profiles in Figure 1 at ${}^{s}_{s}pH$ 11.7 where the equilibrium formation of **7** is far from complete and $[H^+]$ is > (K_B[**5**]) so k_{obs} increases linearly with ${}^{s}_{s}pH$. The Brønsted plot constructed in this ${}^{s}_{s}pH$ region includes the effect of leaving group on both the k_3 term and the equilibrium formation of thiophosphorane **7**. By combining the β_{lg} value of −0.96 ± 0.06 for k_3 (Figure 2) and the β_B value of −1.04 ± 0.17 for log ${}^{s}_{s}K_a^1$ (Figure 8), one gets an overall β_{lg} value of −2.00 ± 0.18, which is gratifyingly close to the β_{lg} value of −1.93 ± 0.06 determined previously.[13]

*4.3.3. Energetics of the Palladacycle **5b**-Promoted Reaction of **6e**.* One way of assessing catalytic efficacy quantifies the free energy difference between the transition state for the methoxide-promoted reactions of **6**, $(MeO^-:\mathbf{6})^{\ddagger}$, and a catalytic transition state comprising **5b**:($^-$OMe):$(HOCH_3)$ plus **6** (or any of its kinetic equivalents such as **5**:$(HOMe)_2$ + $^-$OMe + **6**). This comparison has been used for comparing enzyme and man-made catalyst-promoted reactions relative to the lyoxide promoted background reactions,[27,28] and greatly aided our recent analyses of the origin of the acceleration afforded by a dinuclear Zn(II) complex promoted cleavage of a series of phosphate diesters that are RNA[29a] and DNA[29b] models.

We consider the process given in Scheme 4 with substrate **6e** and the solvated palladacycle **5**:$(HOCH_3)_2$ which does not contain pyridine where the $\Delta\Delta G_{stab}^{\ddagger}$ represents the free energy of binding of the transition state comprising MeO^- + **6e** by the palladacycle: $\Delta G^{\ddagger}_{non}$ and $\Delta G_{cat}^{5\ddagger}$ are the respective free energies of activation of the MeO^- reaction and k_3 rate constant for the cleavage of **7e**, and ΔG_7 is the free energy for formation of **7e** from $^-$OMe, **5**:$(HOCH_3)_2$ and **6**. In eq 13 is the relationship for computing the $\Delta\Delta G_{stab}^{\ddagger}$ where K_B/K_{auto} = [**7e**]/([**5**:$(HOCH_3)_2$][**6e**][$^-$OCH$_3$]); K_B = [**7e**][H^+]/([**5**:$(HOCH_3)_2$][**6e**]) = [**7e**]K_{auto}/([**5**:$(HOCH_3)_2$][**6e**][$^-$OMe]); K_{auto} is the autoprotolysis constant of MeOH ($10^{-16.77}$ M^2) and k_3 is 0.22 s^{-1} from the data in the Supporting Information, Figure 3S.

$$\Delta\Delta G_{stab}^{\ddagger} = (\Delta G_7 + \Delta G_{cat}^{5\ddagger}) - \Delta G_{Non}^{\ddagger} = -RT \ln\left[\frac{(k_3)(K_B/K_{auto})}{k_2^{-OMe}}\right] \quad (13)$$

The formation of **7e** with stoichiometry of **5**:($^-$OCH$_3$):(**6e**) requires palladacycle, methoxide, and **6e**, and the formation

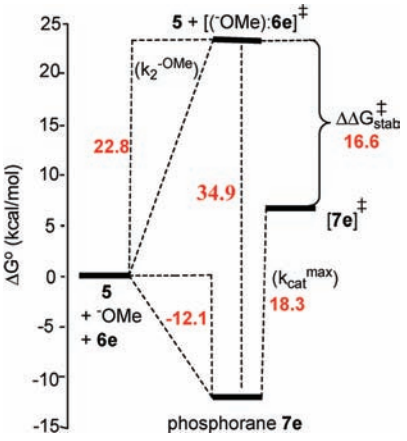

Figure 9. Activation energy diagram for the palladacycle **5**:$(HOCH_3)_2$-catalyzed methanolyses of phosphorothioate **6e** at a standard state of 1 M and 298 K. For simplification, **5**:$(HOCH_3)_2$ is represented in the diagram simply as **5**. The values shown in red include the energies for formation of **5**:($^-$OCH$_3$):(**6e**), (−12.1 kcal/mol); the computed activation energies associated with k_{cat}^{max} (**6e**) (18.3 kcal/mol), and k_2^{-OMe} (22.8 kcal/mol); and the stabilization of the MeO^- + **6e** transition state because of its binding by the palladacycle to form **7e** (34.9 kcal/mol).

constant K_B/K_{auto} = [**7e**]/([**5**:$(HOCH_3)_2$][**6e**][$^-$OMe]) can be numerically obtained as follows. We can determine the K_B/K_{auto} at constant [$^-$OMe] as in each of the three cases used for obtaining the data displayed in Figure 4 with **5**, or for our purposes with **5**:$(HOCH_3)_2$, as in Supporting Information, Figure 3S. There, the K_B/K_{auto} constant can be calculated as K_{cond}/[$^-$OMe] where K_{cond} is a conditional fitting value or binding constant, which gives a K_{dis} of 7.4 × 10^{-5} M at ${}^{s}_{s}pH$ 12.0. The K_{cond}/[$^-$OMe] value is thus 7.95 × 10^8 M^{-2} (or $10^{8.90}$ M^{-2}). The $\Delta\Delta G^{\ddagger}_{stab}$ can be computed in a straightforward way from the various constants as given in eq 13.[30]

One sees in Figure 9 that intermediate **7e** lies −12.1 kcal/mol lower in energy than free palladacycle, methoxide, and substrate **6e**. Part of this comes from the strong binding of the methoxide to the palladacycle, and the subsequent binding and cyclization the substrate to form **7e** lowers the energy of this species further. From the k_3 = 0.22 s^{-1}, one computes the activation energy for P-OAr bond cleavage from **7e** of 18.3 kcal/mol, 6.2 kcal/mol higher than the free energies of reactants at standard state. The $\Delta\Delta G^{\ddagger}_{stab}$ of 16.6 kcal/mol is the difference in energy between the 6.6 kcal/mol and the 22.8 kcal/mol activation energy for the methoxide reaction ($\Delta G^{\ddagger}_{Non}$), and represents one measure of the energy of association of the palladacycle with the [MeO^- + **6e**]‡. Moreover, if we consider that the [MeO^- + **6e**]‡ is phosphorane-like, binding of the palladacycle to that form stabilizes it by 34.9 kcal/mol, converting it into an intermediate. Interestingly, such stabilization of **7e** is so profound that a subsequent step of departure of the leaving group now becomes rate limiting.

5. CONCLUSION

To our knowledge, evidence for metal-ion bound phosphoranes produced along the catalyzed solvolytic pathways for cleavage of neutral acyclic phosphate or phosphorothioate esters does not exist, and it is rare for metal catalyzed cleavage of phosphate diesters and monoesters.[31] In the latter cases, where a

two-step catalytic process for hydrolytic cleavage of phosphate diesters has been experimentally supported, the mechanism is apparently different from that for the hydroxide-promoted hydrolytic reactions which are considered to be concerted. It is an ongoing question whether enzymatic and/or man-made catalysts promote reactions by stabilizing the transition states and intermediates of the background reactions, or by the introduction of new mechanisms.[31,32] This study provides evidence that the palladacycle-promoted methanolysis of neutral phosphorothioates proceeds by a mechanism different than the methoxide-promoted reaction. The background reaction of MeO^- + **6a**−**d** has recently been studied in our laboratories in some detail,[15] and is best described as a concerted process without formation of a detectable intermediate for substrates with good aryloxy leaving groups, and the same appears to be the case from the hydroxide-promoted hydrolytic reactions of phosphorothioate triesters.[22] For these same substrates, the catalytic reaction is multistep with at least two intermediates and the rate limiting step changes as a function of the leaving group from (1) simple displacement of pyridine from **5**:($^-$OCH$_3$)(pyr) by **6a**; to, (2) equilibrium displacement followed by rate limiting intramolecular cyclization to form **7b**−**d** with substrates **6b**−**d**; and then to, (3) equilibrium formation of phosphoranes **7e**−**g** followed by slower cleavage of the P-OAr group. It is of note that all these intermediates had been previously predicted on the basis of our earlier DFT calculations,[13] and the present study points out the predictive success of this sort of computational approach for such processes.

The origin of the large β_{lg} of −1.93 originally seen[13] for the log k_2^{cat} vs $^{s}_{s}pK_a^{HOAr}$ Brønsted plot with poor substrates is now clarified as resulting from two kinetically important steps in which there are substantial changes in the P-OAr bonding. These are the equilibrium steps leading to the Pd-bound thiophosphorane (β_B = −1.04) and rate limiting breakdown of the latter to products (β_{lg} = −0.96), which together give a β_{lg} of −2.00, experimentally the same as the β_{lg} that was found in the previous study. The exact reason for the large value requires more clarification, but we note here that the catalytic process has a Pd-bound nucleophile displacing a free aryloxy group, unlike what is observed for the defining reaction for equilibrium transfer of the dimethyl phosphorothioyl group between oxyanion nucleophiles where the nucleophile and leaving group are free. Large negative β_{lg} values for metal-ion catalyzed phosphoryl transfer reactions may be more general than previously imagined. In contrast to the MeO^--promoted reaction of (EtO)$_2$(ArO)P═O esters which has a β_{lg} value of −0.70, far larger β_{lg} values of −1.43 and −1.12 are observed for their La^{3+} and Zn(II):(1,5,9-triazacyclododecane)-catalyzed methanolyses.[3] Such large values are reminiscent of what is observed for the enzymatic hydrolysis of neutral phosphate triesters and phosphorothioate triesters by a metallophosphotriesterase extracted from the bacterium *Pseudomonas diminuta*.[33−35] There, the enzymatic cleavage of substrates with poor aryloxy leaving groups exhibited large negative Brønsted coefficients of β_{lq} = −2.2 for P═O and β_{lq} = −2.0 for P═S triesters. Earlier we have suggested[3] that the magnitude of large β_{lq} values might result from plotting the kinetic constants vs the pK_a of the leaving group in water. However, the lower effective polarity and dielectric constant inside the enzyme active site might be more representative of an organic solvent like MeOH where the pK_a scales[36] of phenols are expanded, leading to lower values for the actual Brønsted slopes. On the basis of the present palladacycle results, it is also possible that the large $-\beta_{lg}$ values observed for phosphate ester cleavage promoted by the phosphotriesterase enzymes may contain a component attributable to the involvement of metal-ion coordinated phosphorane intermediates.

■ ASSOCIATED CONTENT

Supporting Information. Procedures for kinetic studies; the $^{s}_{s}$pH/rate profiles for the **5d**-catalyzed methanolysis of triesters **6a** and **6c**; spectrophotometric titrations of **5** with NaOMe and methods; initial rate vs [NaOMe] for displacement of pyridine from **5**:($^-$OMe)(Pyr); comparative UV/vis spectra for 0.16 mM each *O*-methyl *O*-phenyl phosphorothioate and **5c**, 8 pages). This material is available free of charge via the Internet at http://pubs.acs.org.

■ AUTHOR INFORMATION

Corresponding Author

*E-mail: rsbrown@chem.queensu.ca. Phone: 613-533-2400. Fax: 613-533-6669.

■ ACKNOWLEDGMENT

The authors gratefully acknowledge the financial support of NSERC Canada, and the U.S. Defense Threat Reduction Agency-Joint Science and Technology Office, Basic and Supporting Sciences Division through the award of Grant HDTRA-08-1-0046. In addition, C.T.L. thanks NSERC for a PGS-2 postgraduate scholarship. We are also indebted to David R. Edwards and Christopher I. Maxwell for helpful discussions concerning aspects of this work and computational results disclosed in ref 13.

■ REFERENCES

(1) (a) Toy, A. D. F.; Walsh, E. N. In *Phosphorus Chemistry in Everyday Living*; 2nd ed.; American Chemical Society: Washington, DC, 1987; pp 18−20; (b) Quin, L. D. In *A Guide to Organophosphorus Chemistry*; Wiley: New York, 2000; pp 367−371.

(2) (a) Tsang, J. S.; Neverov, A. A.; Brown, R. S. *J. Am. Chem. Soc.* **2003**, *125*, 7602. (b) Tsang, J. S. W.; Neverov, A. A.; Brown, R. S. *Org. Biomol. Chem.* **2004**, *2*, 3457. (c) Desloges, W.; Neverov, A. A.; Brown, R. S. *Inorg. Chem.* **2004**, *43*, 6752.

(3) Liu, T.; Neverov, A. A.; Tsang, J. S. W.; Brown, R. S. *Org. Biomol. Chem.* **2005**, *3*, 1525.

(4) Pearson, R. G. *J. Am. Chem. Soc.* **1963**, *85*, 3533.

(5) Parr, R. G.; Pearson, R. G. *J. Am. Chem. Soc.* **1983**, *105*, 7512.

(6) Neverov, A. A.; Brown, R. S. *Org. Biomol. Chem.* **2004**, *2*, 2245.

(7) Ryabov, A. D. In *Palladacycles*; Dupont, J., Pfeffer, M., Eds.; Wiley-VCH: Weinheim, Germany; 2008; pp 307−339; and references within.

(8) (a) Kim, M.; Liu, Q.; Gabbaï, F. P. *Organometallics* **2004**, *23*, 5560. (b) Kim, M.; Gabbaï, F. P. *Dalton Trans.* **2004**, 3403. (c) Kim, M.; Picot, A.; Gabbaï, F. P. *Inorg. Chem.* **2006**, *45*, 5600.

(9) Tao, J. C.; Jia, J.; Wang, X. W.; Zhang, S. T. *Chin. Chem. Lett.* **2002**, *13*, 1170.

(10) Lu, Z.-L.; Neverov, A. A.; Brown, R. S. *Org. Biomol. Chem.* **2005**, *3*, 3379.

(11) (a) Yang, X.-S.; Long, D.-L.; Li, H.-M.; Lu, Z.-L. *Inorg. Chem. Commun.* **2009**, *12*, 572. (b) Lu, Z.-L.; Yang, X.-S.; Wang, R.-Y.; Fun, H.-K.; Chantrapromma, S. *Polyhedron.* **2009**, *28*, 2565.

(12) (a) Lu, Z.-L.; Yang, X.-S.; Guo, Z.-F.; Wang, R.-Y. *J. Coord. Chem.* **2010**, *63*, 2659. (b) Liu, B.-B.; Wang, X.-R.; Guo, Z.-F.; Lu, Z.-L. *Inorg. Chem. Commun.* **2010**, *13*, 814.

(13) Liu, C. T.; Maxwell, C. I.; Edwards, D. R.; Neverov, A. A.; Mosey, N. J.; Brown, R. S. *J. Am. Chem. Soc.* **2010**, *132*, 16599.

(14) For the designation of pH in non-aqueous solvents we use the forms recommended by the IUPAC, *Compendium of Analytical Nomenclature. Definitive Rules 1997*, 3rd ed.; Blackwell: Oxford, U. K, 1998. Thus $^{s}_{s}$pH refers to the measured pH in a non-aqueous solvent references to that solvent. Since the autoprotolysis constant of MeOH is $10^{-16.77}$, neutral $^{s}_{s}$pH is 8.4.

(15) A study of β_{Nuc} and β_{lg} values for the cleavage of substrates **6** gives a β_{eq} value for the transfer of the $(MeO)_2P{=}S$ group between oxyanion nucleophiles of -1.39 ± 0.12 in methanol and -1.45 ± 0.08 in water. (Edwards, D. R.; Maxwell, C. I.; Harkness, R. W.; Neverov, A. A.; Mosey, N. J.; Brown, R. S. *J. Phys. Org. Chem.* In press).

(16) Gibson, G.; Neverov, A. A.; Brown, R. S. *Can. J. Chem.* **2003**, *81*, 495.

(17) Neverov, A. A.; Liu, C. T.; Bunn, S. E.; Edwards, D. R.; White, C. J.; Melnychuk, S. A.; Brown, R. S. *J. Am. Chem. Soc.* **2008**, *130*, 16711.

(18) Tao, W.; Silverberg, L. J.; Rheingold, A. L.; Heck, R. F. *Organometallics.* **1989**, *8*, 2550.

(19) For a two-step process A $\rightleftharpoons$ I $\rightarrow$ P involving reversible formation of an intermediate with breakdown to product, controlled by rate constants k_1, k_{-1}, and k_2, the overall Brønsted plot data of log k_{obs}^{cat} vs $^{s}_{s}pK_a$ can be fit to $k_{obs}^{cat} = k_1k_2/(k_{-1} + k_2) = C_1C_2 10^{(\beta 1+\beta 2)pKa}/(C_{-1}10^{\beta -1pKa} + C_2 10^{\beta 2pKa})$; see Neverov, A. A.; Sunderland, N. E.; Brown, R. S. *Org. Biomol. Chem.* **2005**, *3*, 65.

(20) The model, definition, and use thereof is given as eq (1) in ref 17 and eq (1S) of the Supporting Information.

(21) Edwards, D. R.; Neverov, A. A.; Brown, R. S. *Inorg. Chem.* **2011**, *50*, 1786.

(22) An earlier β_{eq} value for the transfer of $(MeO)_2P{=}S$ group between oxyanions in water was reported to be -0.88 by Omakor, J. E.; Onyido, I.; vanLoon, G. W.; Buncel, E. *J. Chem. Soc., Perkin Trans. 2* **2001**, 324. However, the value was determined from a non-symmetrical reaction where the incoming nucleophile (phenoxide) has a higher pK_a than any of the leaving groups on the substrates. New values for β_{eq} of -1.39 ± 0.12 in methanol and -1.45 ± 0.08 in water are reported in ref 15.

(23) Study of the kinetics of displacement of pyridine from **5b** by 0.01 M $NaOCH_3$ (see Supporting Information) gives a second order rate constant of 5.1 ± 0.2 M^{-1} s^{-1}, while the data of Table 1 for rate-limiting displacement of pyridine from **5b** by 0.05 mM of substrate **6a** gives a value of 0.169 s^{-1}/0.08 mM = 2112 M^{-1} s^{-1}.

(24) $\Delta G^{\ddagger}_{corr}$ values are computed $\Delta G^{\ddagger}$ values with appropriate corrections on the entropic contribution to account for simulation in solvent. Full description and justification are given in ref 13.

(25) While the formation of **7** from involves changes in the bonding of the P-OAr unit, the transition state for cyclization is computed (see Figure 7) to be quite exothermic and early, with a low activation energy from **5**:($^{-}OCH_3$):**6**, accounting from the small or compensatory dependence of the K_1 and k_2 processes on $^{s}_{s}pH_a^{HOAr}$.

(26) (a) Edwards, D. R.; Neverov, A. A.; Brown, R. S. *J. Am. Chem. Soc.* **2009**, *131*, 368. (b) Edwards, D. R.; Garrett, G. E.; Neverov, A. A.; Brown, R. S. *J. Am. Chem. Soc.* **2009**, *131*, 13738.

(27) Wolfenden, R. *Nature* **1969**, *223*, 704.

(28) For analyses using this treatment see Yatsimirsky, A. K. *Coord. Chem. Rev.* **2005**, *249*, 1997 and references therein.

(29) (a) Bunn, S. E.; Liu, C. T.; Lu, Z.-L.; Neverov, A. A.; Brown, R. S. *J. Am. Chem. Soc.* **2007**, *129*, 16238. (b) Neverov, A. A.; Liu, C. T.; Bunn, S. E.; Edwards, D.; White, C. J.; Melnychuk, S. A.; Brown, R. S. *J. Am. Chem. Soc.* **2008**, *130*, 6639.

(30) For rate constants, the values can be calculated as $\Delta G^{\ddagger 5}_{cat} = -RT \ln (k_{cat}^{max}/(kT/h))$ for **6e** and $\Delta G^{\ddagger}_{Non} = -RT \ln(k_2^{-OMe}/(kT/h))$ for the methoxide reaction from the Eyring equation where $(kT/h) = 6 \times 10^{12}$ s^{-1} at 298K.

(31) (a) Williams, N. H.; Cheung, W.; Chin, J. *J. Am. Chem. Soc.* **1998**, *120*, 8079. (b) Humphry, T.; Forconi, M.; Williams, N. H.; Hengge., A, C. *J. Am. Chem. Soc.* **2004**, *126*, 11864. (c) Padovani, M.; Williams, N. H.; Wyman, P. *J. Phys. Org. Chem.* **2004**, *17*, 472. (d) Linjalahti, H.; Feng, G.; Mareque-Rivas, J. C.; Mikkola, S.; Williams, N. H. *J. Am. Chem. Soc.* **2008**, *130*, 4232. (e) Humphrey, T.; Iyer, S.; Iranzo, O.; Morrow, J. R.; Richard, J. P.; Paneth, P.; Henge, A. C. *J. Am. Chem. Soc.* **2008**, *130*, 17858.

(32) Zalatan, J. G.; Herschlag, D. *J. Am. Chem. Soc.* **2006**, *128*, 1293.

(33) Hong, S.-B.; Raushel, F. M. *Biochemistry* **1996**, *35*, 10904.

(34) Donarski, W. J.; Dumas, D. P.; Heitmeyer, D. H.; Lewis, V. E.; Raushel, F. M. *Biochemistry* **1989**, *28*, 4650.

(35) (a) Caldwell, S. R.; Newcomb, J. R.; Schlecht, K. A.; Raushel, F. M. *Biochemistry* **1991**, *30*, 7438. (b) Caldwell, S. R.; Raushel, F. M.; Weiss, P. M.; Cleland, W. W. *Biochemistry* **1991**, *30*, 7444.

(36) Clare, B. W.; Cook, D.; Ko, E. C. F.; Mac, Y. C.; Parker, A. J. *J. Am. Chem. Soc.* **1966**, *88*, 1911.